Heliyon 10 (2024) e31262

Contents lists available at ScienceDirect

Heliyon

journal homepage: www.cell.com/heliyon

Research article

Dust events characterization from visibility, trends and Dust Adversity Index in the Canary Islands for the period 1980–2022

D. Suárez-Molina [a,*], E. Cuevas [b], S. Alonso-Pérez [c,d], L. Cana [e], G. Montero [f], A. Oliver [f]

[a] Territorial Delegation of AEMET in the Canary Islands, State Meteorological Agency of Spain (AEMET), Las Palmas, 35017, Spain
[b] Izaña Atmospheric Research Center (IARC), State Meteorological Agency of Spain (AEMET), Santa Cruz de Tenerife, 38001, Spain
[c] Departamento de Ingeniería Industrial, Universidad de La Laguna (ULL). Avenida San Francisco de Paula, s/n, 38200, La Laguna (Tenerife), Spain
[d] Instituto Universitario de Estudios de las Mujeres. Universidad de La Laguna (ULL), La Laguna (Tenerife), Spain
[e] Unidad Océano y Clima, Instituto de Oceanografía y Cambio Global, IOCAG, Universidad de Las Palmas de Gran Canaria, ULPGC, Unidad Asociada ULPGC-CSIC, Canary Islands, Spain
[f] University Institute for Intelligent Systems and Numerical Applications in Engineering (SIANI), University of Las Palmas de Gran Canaria, Spain

A B S T R A C T

Dust events in the Canary Islands have been documented since the late 19th century. However, during the past few years, several severe dust episodes have occurred in the Canary Islands, resulting in significant impacts on various sectors, such as aviation, air quality, and health, among others. These recent severe events have drawn the attention of both scientists and the general population, raising questions about whether these episodes are now more frequent and more severe. This study analyzes 483 dust events recorded in the Canary Islands over the last 40 years.

Data analysis reveals that the average number of dust event days per year is approximately 24 days, and these events have an average duration of 1.8 days, both of which show a statistically significant decreasing trend over the series. Seasonal examination indicates that events occurring in the first and fourth quarters of the year have twice the duration of those in the other quarters. Furthermore, on an annual basis, events in the first quarter exhibit negative trends in both average and minimum visibilities. This suggests that dust events in the Canary Islands are becoming shorter in duration but more intense in terms of visibility.

In this article, the Dust Adversity Index (DAI) is introduced to objectively compare the severity of events. Finally, anomalies in geopotential have been utilized to determine the prevailing synoptic patterns during dust events. It is evident that the dominant synoptic pattern during the first and fourth quarters of the year consists of a low cut-off system located to the west of the Canary Islands and a high-pressure system to the north of the Iberian Peninsula.

1. Introduction

Desert dust holds significant importance in terms of atmospheric aerosol contributions by mass [1–3]. Various arid regions on Earth serve as sources of this dust, with North Africa accounting for around 50 % of the annual emission and deposition rates of 1.2–3.1 × 10^3 Tg yr^{-1} from all source regions [4,5].

Dust exerts diverse impacts, including risks to human health [6–8], influence on Earth's climate [6,9,10] (; effects on air quality [11,12]), implications for air traffic [13], consequences for agriculture [14], impacts on terrestrial and marine ecosystems [15], and effects on cloud microphysics and precipitation [16]. Given its broad impacts across various socioeconomic sectors and health, significant efforts have been dedicated to enhancing knowledge, monitoring, and forecasting [17]. The World Meteorological

* Corresponding author
E-mail address: dsuarezm@aemet.es (D. Suárez-Molina).

https://doi.org/10.1016/j.heliyon.2024.e31262
Received 26 December 2023; Received in revised form 27 April 2024; Accepted 14 May 2024
Available online 17 May 2024

Organization (WMO) initiated the Sand and Dust Storm Warning Advisory and Assessment System (SDS-WAS) in 2007. Presently, SDS-WAS comprises three regional nodes: (a) North Africa, Middle East, and Europe, (b) Asia and Central Pacific, and (c) Pan-America. These regional centers, facilitated by the SDS-WAS Steering Committee [18], constitute a global network of research, operational centers, and users.

Various variables (such as visibility, concentration, and aerosol optical depth (AOD)) characterize a dust event, and authors like [19,20] have proposed some indices to gauge intensity. However, not all variables possess sufficiently long time series for robust conclusions.

Dust events in the Canary Islands have been documented since the late 19th century [21], which is lógical, given the archipelago's proximity to the primary source of desert dust on Earth [22]. Intrusions of Saharan dust constitute a prominent weather pattern in the Canary Islands [23].

Prior studies have subjectively analyzed favorable atmospheric patterns for desert mineral aerosol transport from North Africa to the Canary Islands [24–34]. These authors generally concur that desert mineral aerosol intrusions in the Canary Islands align with a high-pressure system in North Africa [35] identify three preferred intrusion periods, with winter being the most impactful in terms of air quality deterioration and aeronautical effects.

Given the intensity and impact of recent dust episodes in the Canary Islands (e.g., the February 2020 event; [13]), questions regarding the frequency, intensity, and climate change-related connection of these episodes have arisen from the media, public, social networks, and professionals.

This paper's objectives encompass the characterization of dust intrusions using extended visibility series, analysis of their evolution, seasonal and yearly variations, and trends over the past 42 years. The data comes from the six main Canarian airports, since wer're concerned about the significant impact of reduced visibility on aeronautical operations. The data's length and quality enable firm conclusions. Additionally, due to challenges in objectively assessing dust event severity, an index is will be proposed to gauge intensity quantitatively. Lastly, this study analyzes the synoptic patterns that caused dust events in the Canary Islands from 1980 to March 31, 2022.

The paper's structure involves an introduction to the region of interest and the data in section 2, detailing the methodology. Section 3 delves into results and discussions, followed by the presentation of key conclusions in Section 4.

2. Data and methods

2.1. Area of interest

This study has been conducted within the Canary Islands, an archipelago comprised of 7 islands situated in the subtropical Atlantic, west of Africa, spanning from coordinates 27°37′ to 29°25′ N and 18°10′ to 13°20' W (Fig. 1). These islands are positioned approximately 100 km off the Moroccan coast and 1100 km from mainland Spain. The complex topography of the islands contributes to a diverse climatic range. The higher islands exhibit B, C, and D climatic types [36], while the lower islands, Lanzarote and Fuerteventura, are predominantly characterized by type B climates according to the Köppen-Geiger classification [37].Renowned scholarsauthors like Font Tullot [23,38], in their island-focused publications, have identified 8 primary weather patterns that significantly affect this archipelago. For the analysis of the synoptic patterns (see section 2.3.4), the geographical domain analyzed was (20° N, 50° N; 35° W, 10° E)

For this study, we have employed observational data gathered from the six principal airports across the archipelago: Fuerteventura (GCFV), Lanzarote (GCRR), Gran Canaria (GCLP), Tenerife Norte (GCXO), Tenerife Sur (GCTS), and La Palma (GCLA).

2.2. Data

2.2.1. Observation data

We have used visibility data derived from the 13 UTC (Universal Time Coordinated) surface synoptic observations (SYNOP) together with relative humidity measurements from the six airports. The data spans from January 1, 1980, to March 31, 2022. The quantification of visibility aligns with the protocols defined by the World Meteorological Organization, as stipulated in Refs. [39,40]. Likewise, relative humidity has been measured through HMP155 sensor models manufactured by Vaisala.

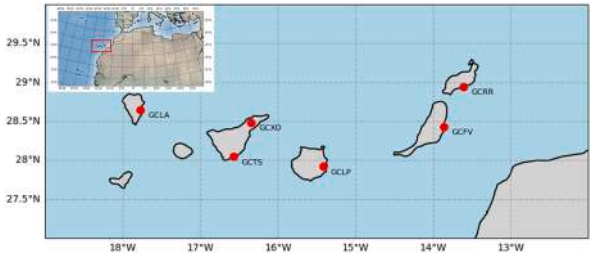

Fig. 1. Area of interest. Red box highlights the Canary Islands. On the islands the location of the airports is marked with their indicatives. (For interpretation of the references to colour in this figure legend, the reader is referred to the Web version of this article.)

These data sets have been sourced from the National Climatic Data Bank, administered by the State Meteorological Agency of Spain (AEMET). It is important to note that rigorous validation procedures have been employed to ensure the accuracy and reliability of the data.

2.2.2. Reanalysis data

To identify the most frequent meteorological patterns that encourage African dust intrusions over the Canary Islands, daily reanalysis daily of geopotential height anomalies at 925, 850, 700 and 500 hPa are used. The data comes from the NCEP/NCAR Reanalysis 1 project [41] provided by the National Centers for Environmental Protection (NCEP) and the National Centre for Atmospheric Research (NCAR). The standard reference climatology time period for the anomalies calculation is 1991–2020. The geopotential height anomalies are calculated as the difference between the geopotential height daily mean for a certain day and the geopoptential height monthly mean of the corresponding month for the standard reference period. The spatial resolution is $2.5^{\circ} \times 2.5^{\circ}$.

2.3. Method

2.3.1. Dust event definition

In this study, a "dust event" occurs when the presence of dust reduces the horizontal visibility to less than 10 km in at least two aerodromes simultaneously. This ten kilometres threshold is chosen because it is the one used in METAR (Meteorological Aerodrome Report) and TAF (Terminal Aerodrome Forecast) reports [42]. To determine if the visibility reduction is due to dust, we consider that a relative humidity measurement below 70 %. This threshold is introduced to exclude possible influence of fog or mist events, thus ensuring that the reduction in visibility is due to dust.

2.3.2. Trend analysis

We use the Mann-Kendall test [43–45] to detect potential trends within the time series data. This statistical test, widely adopted for environmental time series analysis [46], evaluates the rejection of the null hypothesis (H0) in favor of the alternative hypothesis (Ha). The null hypothesis states the absence of a monotonic trend, while the alternative hypothesis asserts its presence. The R package "Kendall" is utilized, with a significance level set at $\alpha = 0.05$.

2.3.3. Dust Adversity Index (DAI)

The adversity of a dust event in an area of interest is determined by the reduction in visibility (there is a relationship between visibility and dust mass concentration, see for exemple [47]), the affected area (number of affected stations) and the persistence of the event (number of days of duration). It is easy to find precipitation records that have been measured in a specific place, or the extreme temperatures registred for a specific location. However, it is more complex to determine a ranking of dust events based on their intensity in an area of interest.

Severity indices can be found in the literature to determine the intensity of dust events [48–50]. These indices have some limitations, as some of them only take visibility into account, or in other cases they are based on AOD, or they are based on number of affected stations and visibility. However, none of them contain information on dust concentration, area affected and persistence of the event. This is the reason why we introduce the Dust Adversity Index (DAI), with the aim of encapsulate key characteristics of dust events and facilitate comparisons between different occurrences to ascertain their relative adversity.

The DAI is defined as shown in equation (1):

$$DAI = s/s_T * x/x_r * d * 10^4/v_m \quad (1)$$

Where.

- "s" represents the number of stations affected by the dust event, with potential values ranging from 2 to 6. The role of "s" in the index is to take into account that the greater the number of affected stations, the evidently the dust event has a less local character and is more widespread.
- "s_T" is the total number of stations in the area of interest. For the present study, s_T is equal to 6.
- "d" is the duration factor, which takes values between 1 and 5 determined by percentiles of the dust event duration. This tabulation is done to minimize the impact on the DAI of the outlaiers. Table 1 shows the relationship.
- "V_m" is mean visibility of dust event in m. It is calculated as the average of the visibility of all stations during the entire event.

Table 1
Values of the "d" parameter as a function of the percentile of the dust event duration.

Dust event duration (in days)	d value
1–2	1
3(P72) - 4(P86)	2
5 (P95)	3
6-8 (P98)	4
>8 (P99)	5

- "x/x_r" To guarantee comparability of results across various regions, we have introduced a term that represents the maximum separation distance between the analyzed stations. In this study, we use the variable "x" to denote the maximum distance between the furthest stations, while "x_r" represents the reference distance (xr = 406.79 km), which corresponds to the distance between GCRR and GCLA. Therefore, in our case, the ratio "x/xr" is equal to 1.

2.3.4. K-means

The K-means clustering algorithm, as introduced in Ref. [51], is a widely recognized and robust technique employed for the categorization of data into distinct clusters.We use this algorithm to calculate the main patterns of geopotential height anomalies in the area and time period of study, for all the tropospheric levels considered, and grouping the days of dust events into four quarters. We adopt a methodological approach similar to the one employed in Ref. [34].

3. Results and discussion

Using the methodology outlined in section 2.3.1, an examination spanning from 1980 to 2022 reveals a total of 483 instances of dust events in the Canary Islands. Among these occurrences, 46 events exhibit an average visibility of 5000 m or less.

It is worth noting that of the 46 events with an average visibility equal to or lower than 5000 m, only 9 dust events (1983-01-17; 1983-12-27; 1988-12-27; 1992-01-03; 1998-02-12; 2004-03-03; 2013-02-04; 2020-02-22; 2022-01-28) affected the 6 main airports of the Canary Islands. As shown in Fig. 2, these events had a different duration but were characterised by their intensity (low average visibility) and their wide extension (all stations were affected). As will be shown in section 3.2 variously, within these 9 dust events are the most intense ones.To encapsulate these 46 events, Fig. 2 serves as an illustrative summary. The height of the bar represents the event's average visibility, while the width represents its duration. Each bar is accompanied by a label denoting the number of airports influenced by the event.

3.1. Basic statistics and trend tests

To present and analyze all the dust events, we group them into five distinct periods. The first one, the Annual group, includes all the data. The other four are grouped by quarters: Q1 includes all the dust events that occurred during January, February, and March; Q2 has all the events that happened during April, May, and June; Q3 has all the events that happened during July, August, and September; and finally, Q4, has all the events that happened during October, November, and December.

For each group, we want to analyze the duration of the events, their visibility (both mean and minimum values), and the number of days of dust events in the period. Table 2 shows the mean, median, standard deviation (SD), the slope of trends (τ), and the p-value of all these values for each group. The slope of the trends (τ) distinguishes between rising ($\tau > 0$) and falling ($\tau < 0$) trends. The p-value detects statistically significant trends; greyed rows represent the significant ones ($p < \alpha$).

Following, we present an in-depth analysis of each group.

3.1.1. Annual analysis

In the study period there have been 24.12 ± 12.15 (with a median of 22.50 days per year) days of dust events annually. The average

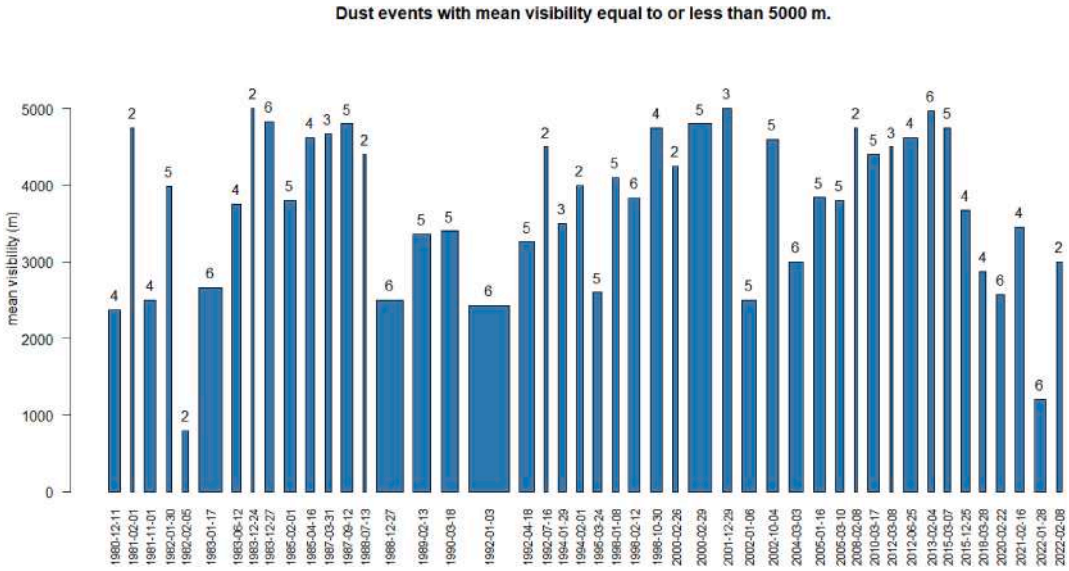

Fig. 2. Summary of the 46 most intense dust events that occurred in the Canary Islands (average visibility equal to or less than 5000 m).

Table 2
Statistical results and trend test for different periods. (January, February, and March (Q1); April, May and June (Q2); July, August and September (Q3) and October, November and December (Q4)).

	mean	median	sd	Ƭ	p-vaule
Annual duration (days)	1.81	1.8	0.35	-0.238	**0.028343**
Annual mean visibility (m)	8141	8069	640	-0.157	0.14644
Annual mínimum visibility (m)	7165	7094	832	-0.123	0.25507
Number of annual dust event days	24.12	22.50	12.15	-0.627	**7.28E-05**
Q1 duration (days)	1.93	1.8	0.91	-0.158	0.14679
Q1 Mean visibility (m)	7359	7339	1410	-0.115	0.28103
Q1 minimum visibility (m)	6062	6033	2012	-0.0958	0.37334
Q1 days of dust events	8.42	8	4.92	-0.205	0.060002
Q2 duration (days)	1.44	1,.58	0.81	-0.278	**0.013941**
Q2 Mean visibility (m)	9085	9242	912	0.172	0.12074
Q2 mínimum visibility (m)	8531	8708	1383	0.124	0.27177
Q2 days of dust events	4.02	3.50	3.05	-0.433	**0.00010466**
Q3 duration (days)	1.85	1.95	0.97	-0.375	**0.00063657**
Q3 Mean visibility (m)	8964	8881	694	0.061	0.57979
Q3 mínimum visibility (m)	8011	8000	1193	-0.0771	0.48647
Q3 days of dust events	8.10	7	6.45	-0.528	**1,45E-02**
Q4 duration (days)	1.30	1.50	0.87	0.078	0.50065
Q4 Mean visibility (m)	8190	8333	1554	0.0661	0.55447
Q4 mínimum visibility (m)	7149	7500	2344	0.0836	0.45629
Q4 days of dust events	3.07	3	2.68	-0.165	0.14686

duration of these dust events over the years is 1.81 ± 0.35 days (with a median of 1.80 days). The annual mean (median) visibility is 8141 ± 640 m (8069 m), and the annual mean (median) minimum visibility is 7165 ± 832 m (7094 m). During this period, both the number of days with dust events and the duration of these events have decreased, with Ƭ values of −0.627 and −0.238, respectively, as indicated by the results of the trend test (see Table 2 and Fig. 3). These trends are statistically significant at a significance level of $\alpha = 0.05$. Despite these downward trends, annual variability is observed. The results obtained here are in line with previous studies [52, 53]. These studies examine the annual trends and variability of dust over North Africa. The authors state that periods favorable for dust production, such as the late 1980s, are caused by abnormally high winds and low soil moisture [6,54,55]. According to Ref. [53], the decreasing trend observed between 1986 and 2000 was due to a decrease in wind intensity and an increase in soil moisture, which contributed to dust suppression. Since 2011, there has been an increase in dust activity in North Africa. This can be attributed to a

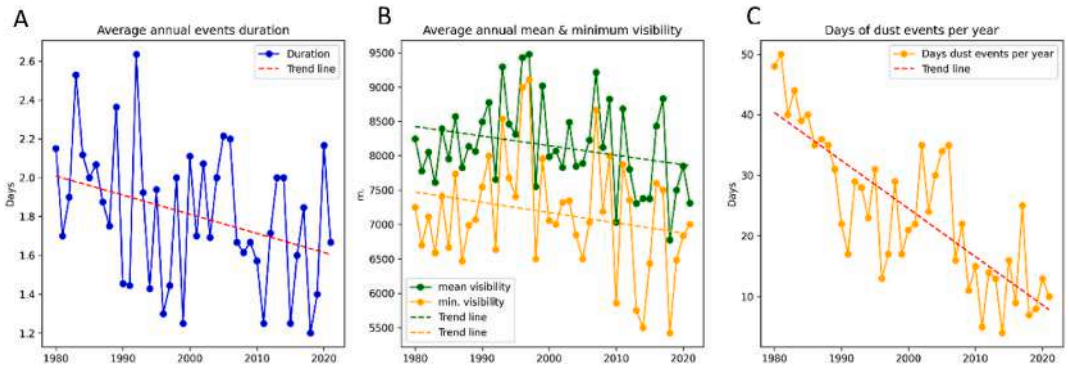

Fig. 3. Annual evolution of the variables: A) Annual average duration of dust events. B) Annual average of mean and minimum visibility. C) Number of days of dust events.

decrease in soil moisture and an increase in wind intensity [53].

The annual average visibility (both mean and minimum visibility) has shown negative trends. This suggests that the events have become more intense, resulting in further reductions in visibility. However, these trends are not statistically significant.

3.1.2. Monthly analysis

Fig. 4 depicts the monthly average of the duration and the visibility (mean and minimum). The longest events occur in January and February, spanning 2.10 and 2.11 days, respectively. In contrast, the shortest dust events manifest in November, lasting 1.48 days. Regarding visibility, the most intense events occur in February, December, and January, with mean visibility levels of 6963, 7101, and 7252 m, respectively. However, the minimum visibility levels occur in December, February, and October, with values of 5550, 5563, and 5708 m, respectively. Analyzing both the mean and minimum visibility values we can conclude that the least intense dust events occur from April to September.

3.1.3. Seasonal analysis

A first analysis of Table 2 and Fig. 5 shows us that, on average, there are twice as many occurrences in the Q1 and Q3 quarters as in the other two quarters. In Q1 and Q3 the occurrence is slightly higher than 8 days (8.42 and 8.10 respectively), while in Q2 and Q4 the values are between 3 and 4 days (4.02 and 3.07). The analysis of the average visibility reveals that the most severe events occur in the Q1 quarter, with an average visibility of 7359 $\pm$ 1410 m. In contrast, the least affected quarter is Q2, with an average visibility of 9085 $\pm$ 912 m. The above is also consistent when examining the average minimum visibility, where the Q1 quarter also presents the most reduced visibility with an average of 6062 $\pm$ 2021 m.

Considering the τ, it is discernible that all variables exhibit negative values during the Q1 quarter, suggesting shorter yet more intense events. However, the trends lack statistical significance at a confidence level of $\alpha = 0.05$. In the Q2 quarter, events show a negative τ in duration and days of occurrence, but a positive τ in visibility (both mean and minimum). Noteworthy is the statistical significance of the duration and days of occurrence trends during this quarter. For Q3, significant negative τ manifest in duration and event days, while visibility τ diverge with mean visibility showing an upward trend and minimum visibility showing a downward trend. In contrast, the τ for visibility variables (mean and minimum) remain statistically insignificant during the Q1 quarter. During Q4, all variables except the number of event days show a positive trends. However, these trends lack statistical significance.

To complete the seasonal analysis of dust events in the area of interest, the methodology of section 2.3.4 has been applied to determine the synoptic patterns during dust events occurring in each quarter. During the first quarter (Fig. 6), dust events manifest under the influence of a well-defined dipole pattern characterized by a low cut-off (more profound in 52 % of instances, clusters 2 and 4) to the western region of the Canary Islands, juxtaposed with a high-pressure system centered to the north-northeast of the Iberian Peninsula at the 500 hPa level.

Across the other atmospheric levels (700 hPa, 850 hPa, and 925 hPa), the meteorological configuration exhibits parallels, although the drop in height is less marked in the lower levels of the troposphere. This atmospheric pattern generates an east-southeast flow at lower altitudes, facilitating the transport of mineral-laden desert aerosols from the African landmass into the Atlantic domain. The interplay with the low-pressure cutoff positioned to the west of the Canary Islands moves the dust particles upwards, subsequently entrapping them. This phenomenon forces a recirculation of air over the islands Cuevas et al. (2021) concluded that this weather pattern produces the most severe dust events in the Canary Islands. Due to the significance of this pattern in dust episodes in the Canary Islands, it will be referred to in the following quarters.

During the second quarter (Fig. 7), a high-pressure system is present either in the northwest (approximately 82 % of the time) or in the west (approximately 18 %) of the Iberian Peninsula at the 500 hPa atmospheric level.Furthermore, the geopotential anomalies are less marked at the 925 hPa level, except within cluster 1 (approximately 33 %), where the high-pressure configuration mirrors the customary disposition observed at the 500 hPa level.

In this quarter, only a situation similar to the predominant one in Q1, a dipole of low pressure (located west of the Canary Islands) and high pressure (located north of the Iberian Peninsula), appears at the 850 hPa level (approximately 46 % of events).

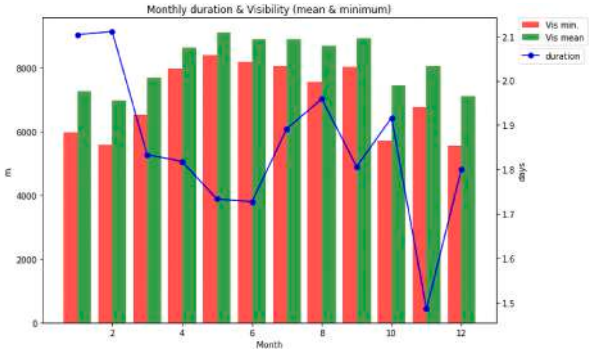

Fig. 4. Monthly average of duration (blue line), mean (green bar) and minimum visibility (red bar). (For interpretation of the references to colour in this figure legend, the reader is referred to the Web version of this article.)

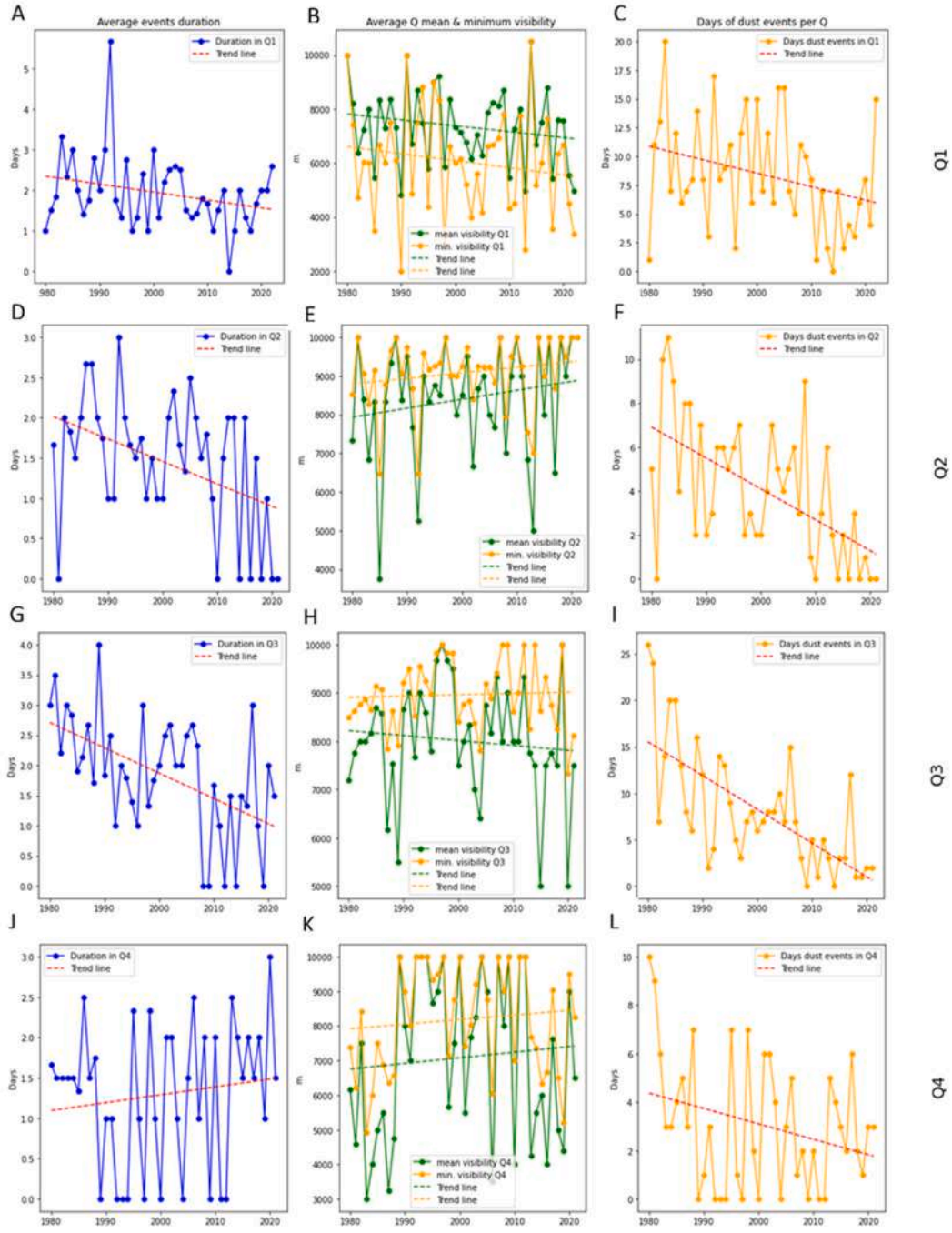

Fig. 5. Quarters evolution of the variables: Average duration of dust events [A, D, G, J]. Average of mean and minimum visibility [B, E, H, K]. Number of days of dust events [C, F, I, L]. Each row corresponds to the quarter indicated on the right (Q1, Q2, Q3, Q4).

During the third quarter (Fig. 8), the geopotential anomalies at the different levels are, in general, less marked than in the other quarters. At the 500 hPa level, it is observed that approximately 65 % of instances are characterized by a dominant positive geopotential anomaly positioned to the north-northwest of the Iberian Peninsula. Within cluster 4 (approximately 19 %), negative geopotential anomalies manifest over the African continent and the southwestern vicinity of the Azores.

The pattern discernible at the 700 hPa level closely resembles that observed at 500 hPa, albeit with the positive geopotential anomalies (Clusters 1 and 4) centered slightly further south. At the 850 hPa level, around 78 % of dust events display inconspicuous geopotential anomalies. Notably, about 22 % (cluster 2) of occurrences in this quarter exhibit dust events transpiring in the presence of a robust anticyclonic system located within the subtropical Atlantic. A parallel circumstance is mirrored at the 925 hPa level, wherein

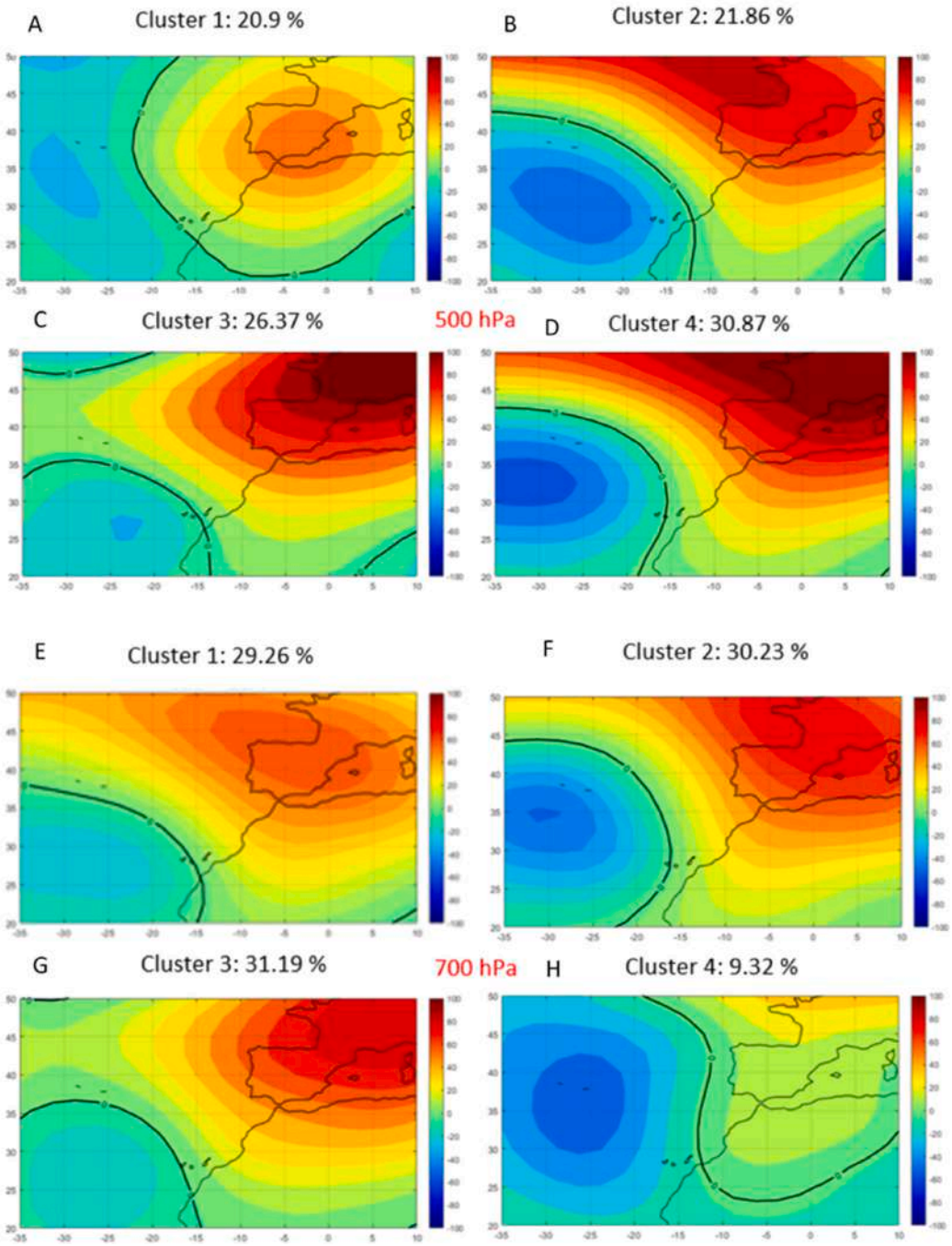

Fig. 6. Clusters of main patterns of geopotential height anomalies for different atmospheric levels and for Q1. [A-D] Panels corresponding to the 500 hPa. [E-H] Panels corresponding to the 700 hPa. [I-L] Panels corresponding to the 850 hPa. [M – P] Panels corresponding to the 925 hPa.

negligible geopotential anomalies are observed throughout this quarter.

During the fourth quarter (Fig. 9), the geopotential anomalies are more noticeable and the high-low dipole structure can be seen in a large part of the middle and lower troposphere (similar to Q1). At 500 hPa, positive anomalies centered north of the Iberian Peninsula are observed in most of the dust events, except for ≈9 % (cluster 4) that appear centered north of the Azores. At this level, the negative geopotential anomalies are centered to the west of the Canary Islands. The low-high dipole interaction produces an intense south-easterly flow that favors aerosol advection from the source region to the Canary Islands.

As we descend in levels, it is observed how the negative geopotential anomalies centered to the west of the Canary Islands decrease

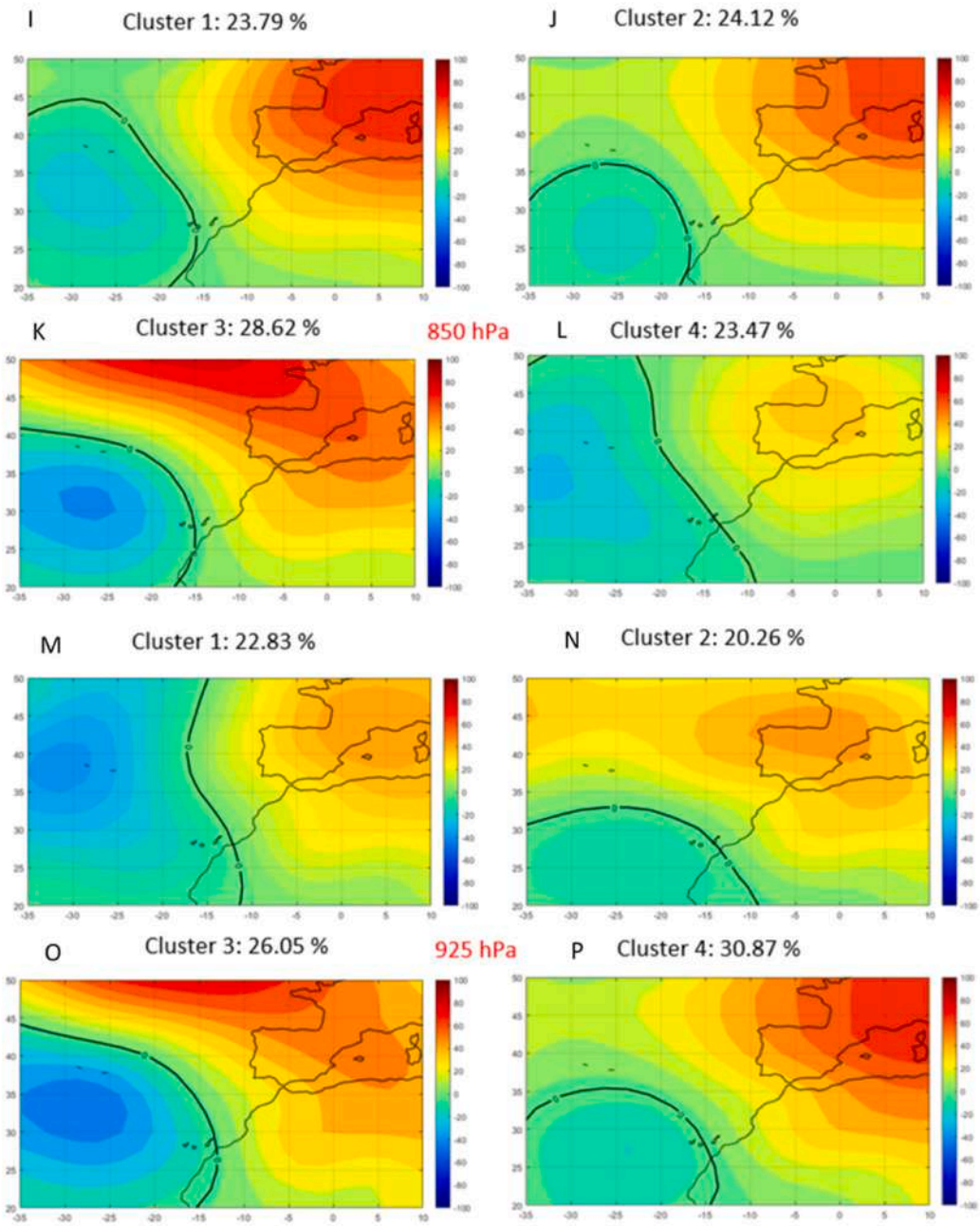

Fig. 6. (*continued*).

in intensity. This is because the systems present during dust events are low cut-off.

Thus, it can be seen that at the 700 hPa level the marked negative geopotential anomalies in the Canary Islands are 50 % (Clusters 3 and 4), 45 % (Clusters 1 and 3) at 850 hPa and 19 % (Cluster 1) at 925 hPa.

3.2. *Dust Adversity Index (DAI)*

Fig. 10 shows the Dust Adversity Index (DAI) values encompassing 483 dust events in the period of interest. The mean value of the DAI stands at 1.27, with the following distribution: 466 occurrences exhibit DAI values of 5 or less, 13 have values between 5 and 10, and only four have values above 10. These four instances are March 1, 1992; December 27, 1988; January 17, 1983; and January 28, 2022 (in descending order of DAI mean value). As the results show, three of the four most intense dust events, based on DAI, have

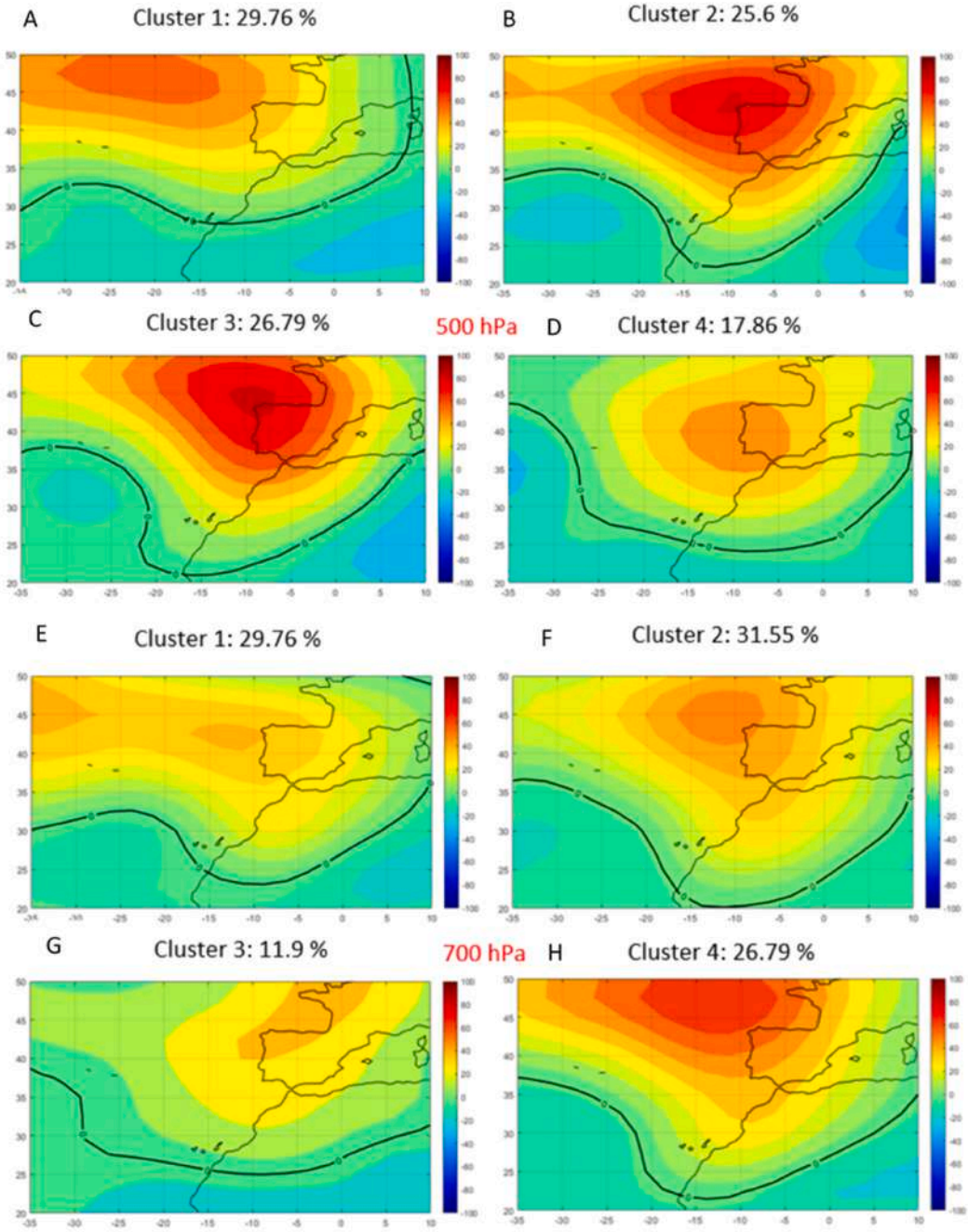

Fig. 7. Clusters of main patterns of geopotential height anomalies for different atmospheric levels and for Q2. [A-D] Panels corresponding to the 500 hPa. [E-H] Panels corresponding to the 700 hPa. [I-L] Panels corresponding to the 850 hPa. [M – P] Panels corresponding to the 925 hPa.

occurred during Q1. This is due to the seasonality of the SAL and the characteristics shown by the desert aerosol intrusions during Q1 in the Canary Islands. In this quarter, the dust intrusions are characterised by the continental air mass replacing the maritime air mass associated with the trade winds due to the eastward displacement of the Azores anticyclone. During these situations, the strong easterly wind in the lower levels of the troposphere causes high concentrations of dust to travel from low levels from the source region to the area of interest, affecting the Canary airports.

Analyzing the annual DAI mean value (shown in Fig. 11), we conclude that most years have values between 0.5 and 2. On the extremes, two years have values below 0.5: 2011 (0.39) and 1996 (0.45), and three years above 2: 1992 (3.02), 1983 (2.47), and 1989 (2.11).

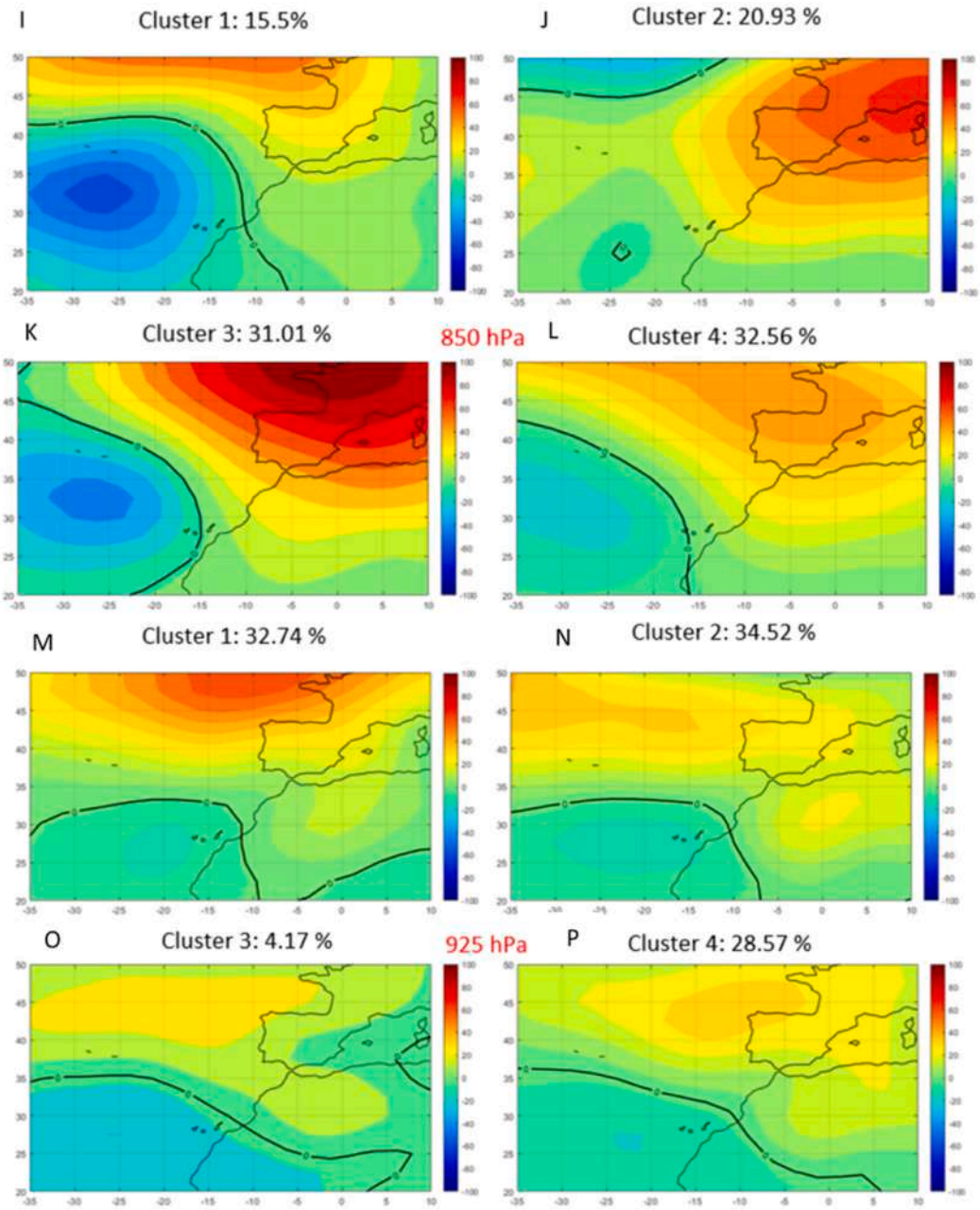

Fig. 7. (*continued*).

Fig. 12 exhibits the monthly mean values of the DAI. The severity of dust events is more pronounced during the winter months, leading to elevated DAI values. This pattern is particularly prominent in January, which boasts the highest monthly mean DAI of 2.42, while the lowest value is observed in May, standing at 0.56.

Fig. 13 offers a depiction of the temporal evolution of DAI from January 1980 to March 2022. The average DAI values for each quarter are 1.79, 0.69, 0.75, and 0.92 for Q1, Q2, Q3, and Q4, respectively and this is consistent with the DAI values obtained in the monthly analysis. The seasonal analysis of DAI shows that throughout the study period, exceeding the DAI threshold of 3 occurred more frequently in Q1 than in the other quarters. Specifically, in the Q1 of the years 1992, 1990, 2022, 1983, 1985, and 2004 (arranged in decreasing order of DAI values), DAI exceeded 3. For Q2, DAI was higher than 3 in 1992, while for Q3 and Q4, it exceeded this threshold in 1989 and 1988, respectively. As the results show, the events that occurred in Q1 are, in general, more intense than in the rest of the year. The above is consistent with other studies carried out in the area of interest [56] and is caused by the seasonal variation in the vertical structure of the Saharan Air Layer (SAL) [57] and in the synotic patterns.

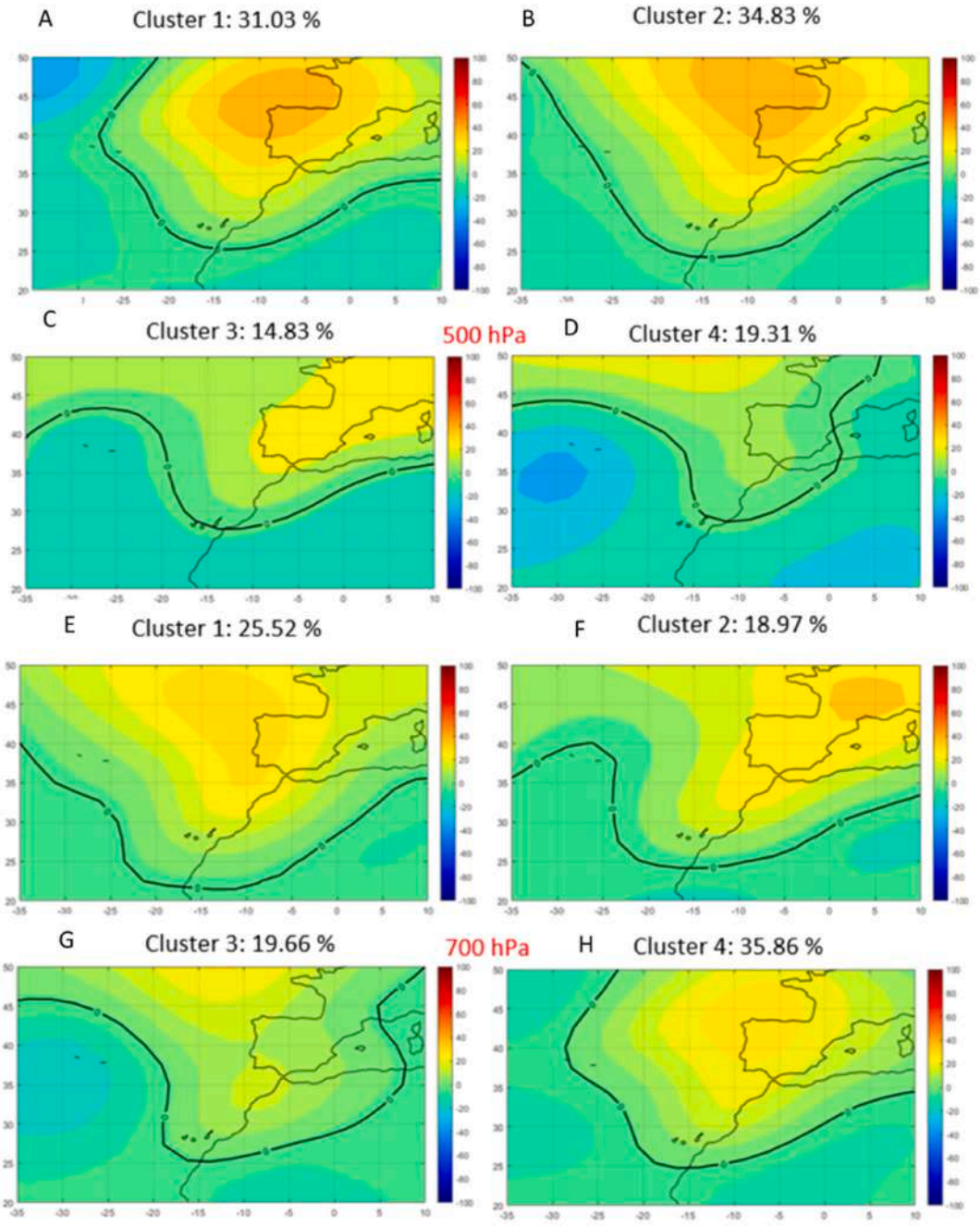

Fig. 8. Clusters of main patterns of geopotential height anomalies for different atmospheric levels and for Q3. [A-D] Panels corresponding to the 500 hPa. [E-H] Panels corresponding to the 700 hPa. [I-L] Panels corresponding to the 850 hPa. [M – P] Panels corresponding to the 925 hPa.

3.3. Case study

To further validate DAI in other regions, DAI was calculated for another study area during an intense dust event. Four stations located in northwest Africa were selected for this purpose: GMML, Laayoune/Hassan Isl (Morocco); GMAD, Agadir Al Massira (Morocco); GMMI, Essaouira - Mogador Intl. Airport (Morocco); and DAOF, Tindouf (Algeria). In this case study, a dust event occurred from 21 to February 25, 2020, lasting for 5 days, which is longer than the 3-day event in the Canary Islands. The average visibility during the event was 6000 m, and the maximum distance between stations was 595.75 km, resulting in an x/x_r value of 1.46.

The DAI value for this case study's dust event is 7.3, while for the Canary Islands event, it is 7.79. Although DAI was applied to areas

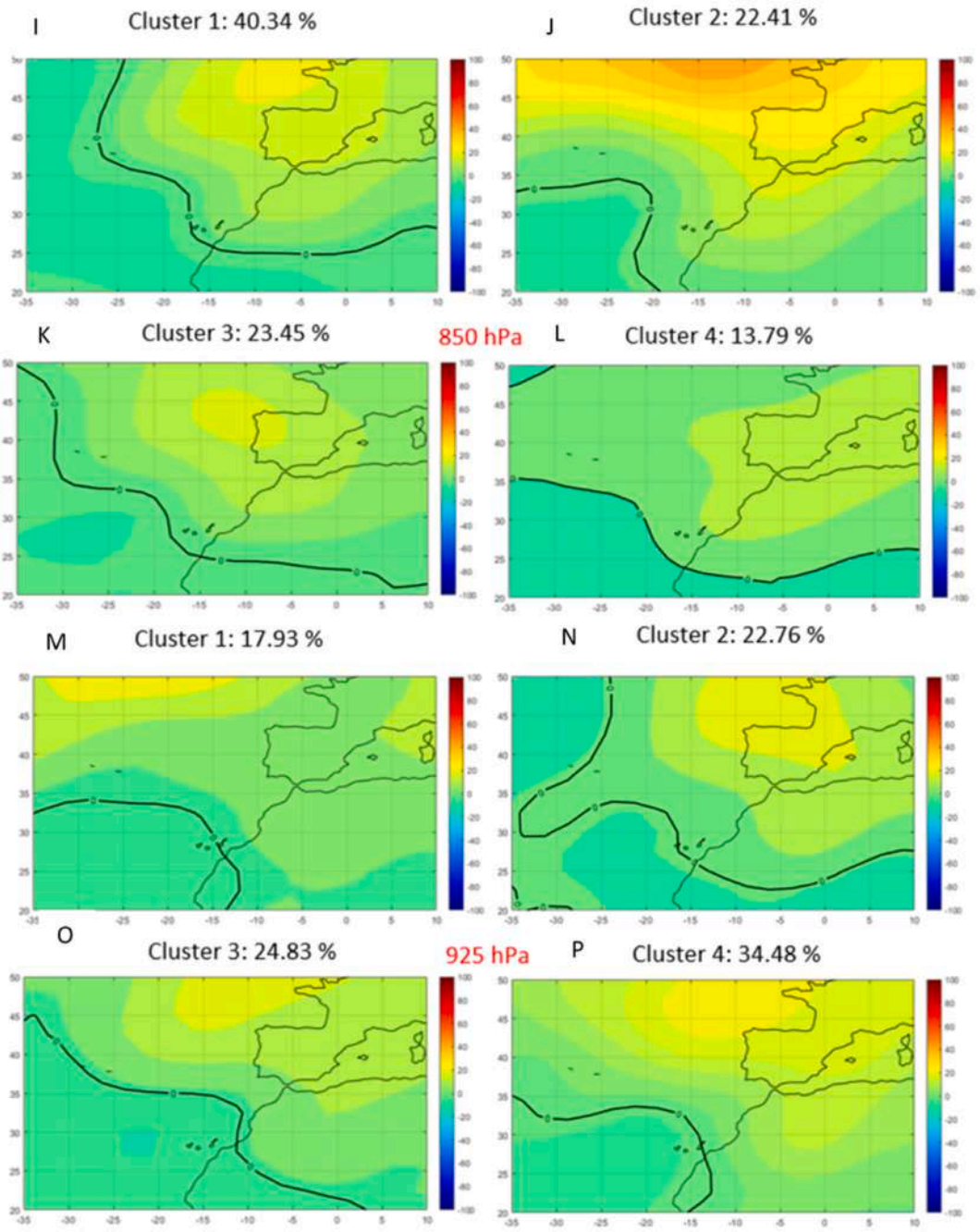

Fig. 8. (*continued*).

of varying characteristics, such as distance between stations and number of stations, the resulting DAI values were similar. This shows the usefulness of DAI in determining the intensity of dust events in different areas and characterising them objectively based on relevance criteria such as visibility, persistence, and affected area. This approach can help us better understand the impact of dust events on different areas and take appropriate measures to mitigate their effects.

4. Conclusions and summary

This article has analyzed the dust events that have affected the Canary Islands during the period between 1980 and 2022. The study encompasses the characterization of dust events across various timeframes and the exploration of trends in key variables of interest,

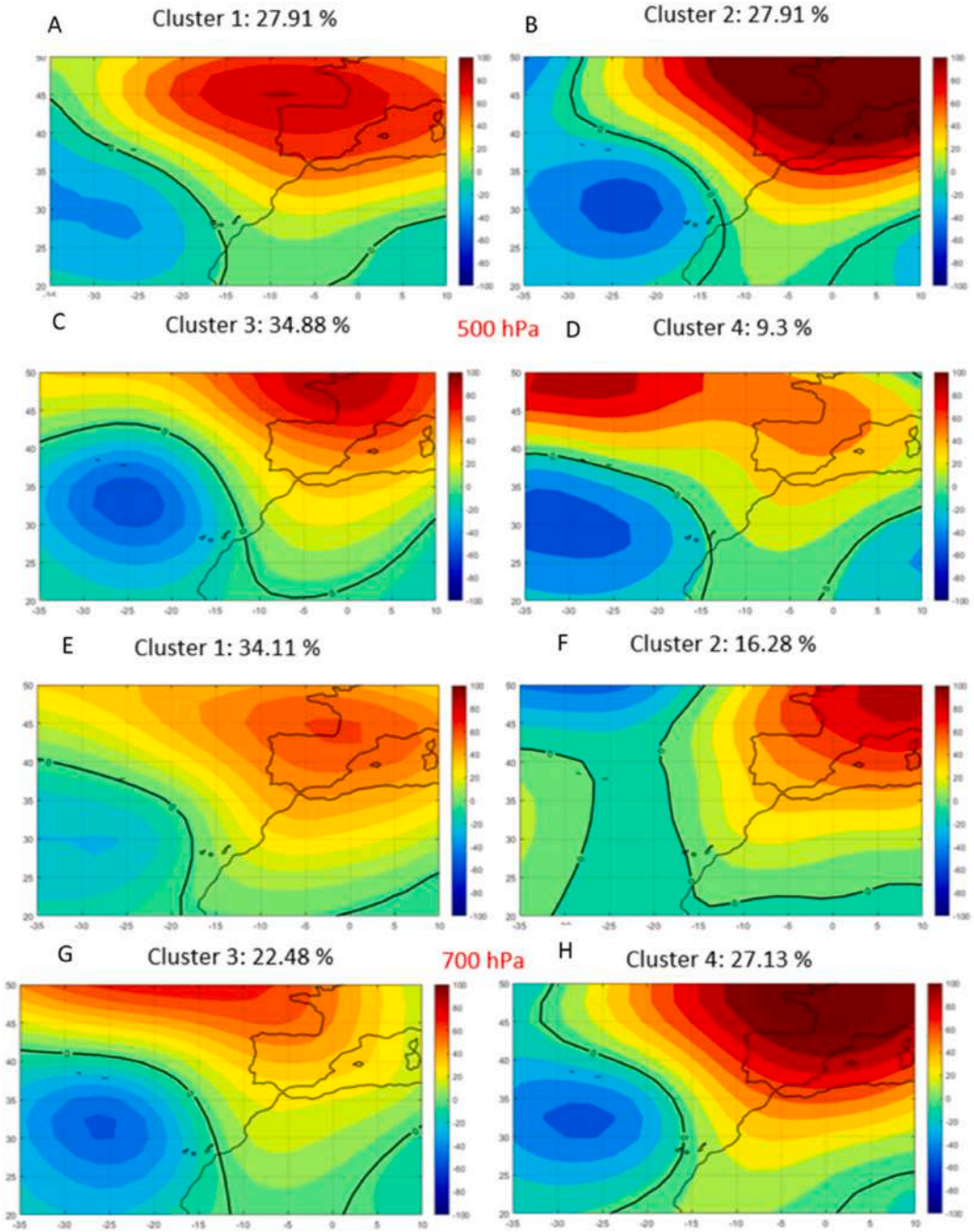

Fig. 9. Clusters of main patterns of geopotential height anomalies for different atmospheric levels and for Q4. [A-D] Panels corresponding to the 500 hPa. [E-H] Panels corresponding to the 700 hPa. [I-L] Panels corresponding to the 850 hPa. [M – P] Panels corresponding to the 925 hPa.

encompassing factors such as event duration, mean visibility, minimum visibility, and event duration.

With the aim of improving the deficiencies found in other severity indices, this article proposes an index (DAI) that objectively allows knowing and comparing the intensity of each dust event In addition, we analyze the prevailing weather patterns that favor desert mineral dust intrusions from source regions and trigger dust events in the Canary Islands.

The main findings of this study are the following.

- A total of 483 dust events have been documented in the Canary Islands between 1980, and 2022. Among these, only 9 events affected all the 6 main airports with an average visibility of less than 5000 m.

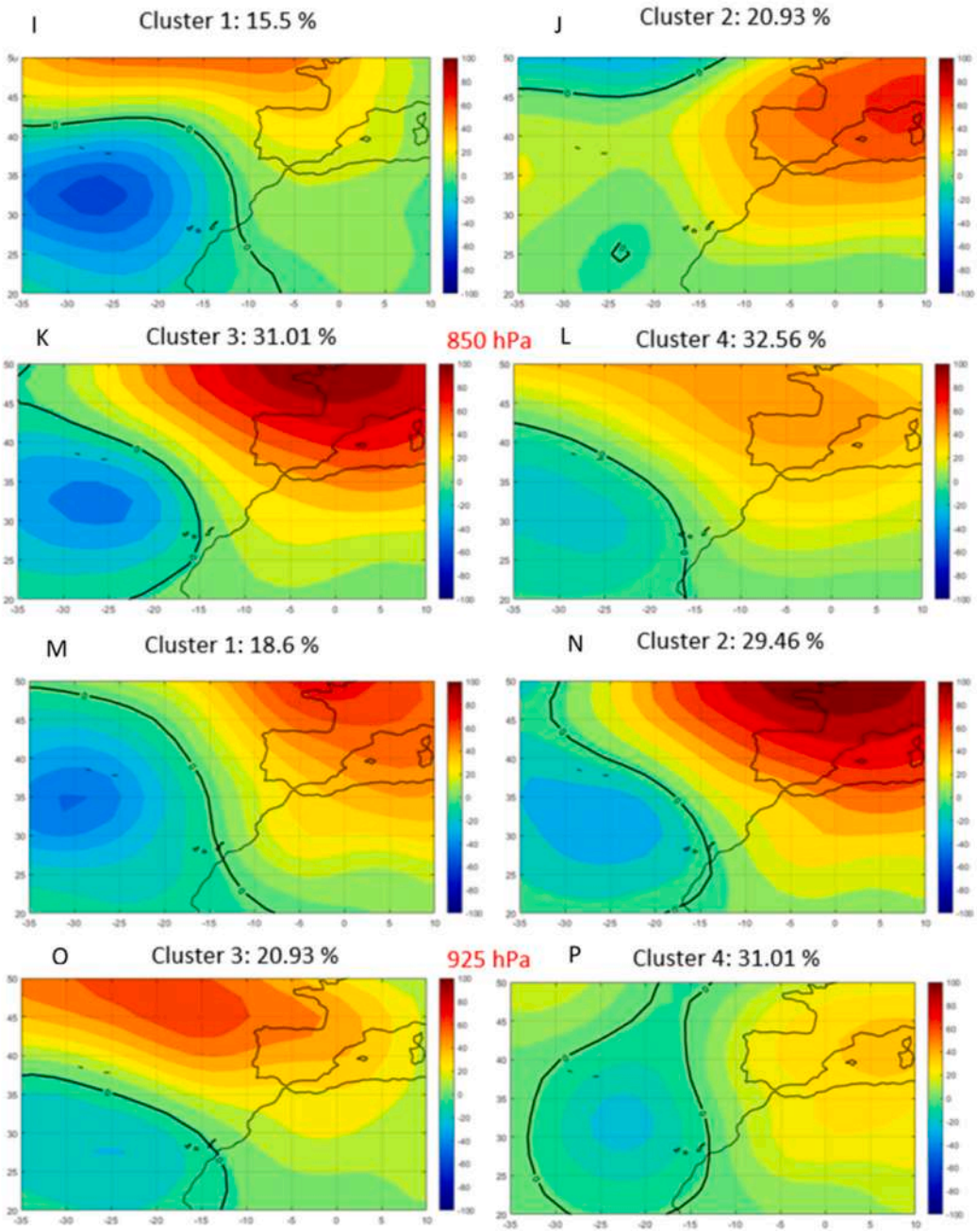

Fig. 9. (*continued*).

- Annual analysis reveals that the variables concerning the number of days and event duration have exhibited a statistically significant decline over the study period. As for visibility-related variables (average and minimum), negative trends indicate heightened event intensity; however, statistical significance is not observed.
- The monthly analysis has revealed that the longest dust events occur in the months of January and February, and that in addition, the events that reduce visibility the most, on average, occur in February. Conversely, the shortest events occur in November and the smallest reductions in visibility occur between April and September.
- The seasonal analysis shows that the longest and most intense events in terms of reduced visibility (medium and minimum) occurred in the Q1 quarter. Trends were analyzed quarterly. This analysis indicates downward and statistically significant trends in the AMJ and JAS quarters for the variables duration and days of dust events. The synoptic patterns prevailing during dust events are investigated via k-means clustering, using geopotential anomalies at distinct tropospheric levels. In the first and fourth quarters, the dust events occur when the dominant synoptic pattern exhibits a prominent high-low dipole structure. Specifically, the high-

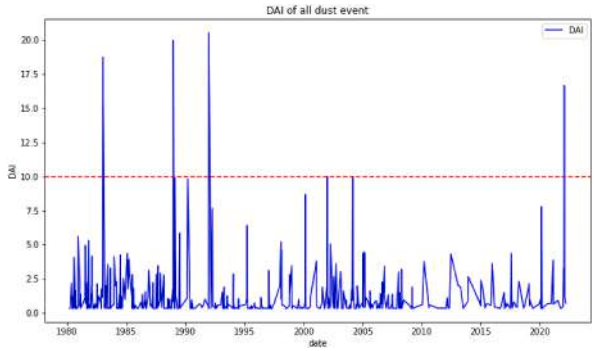

Fig. 10. DAI of all dust events analyzed (483 dust events) in the Canary Islands during the period of interest.

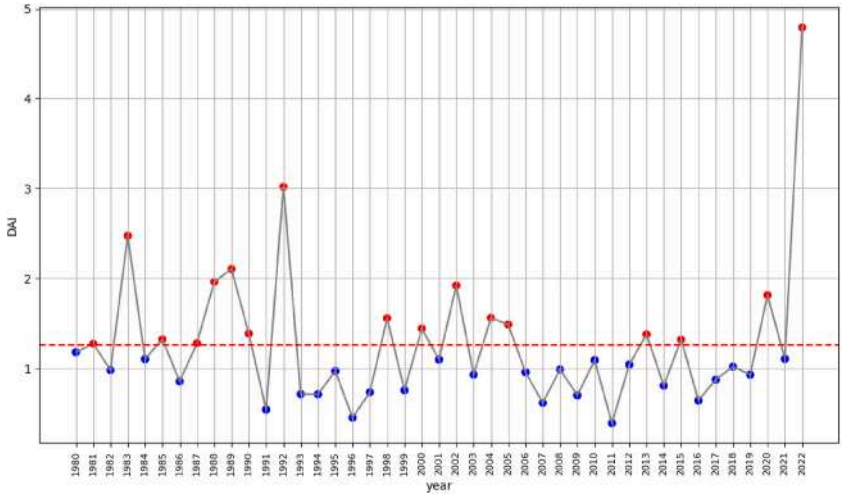

Fig. 11. Annual average of DAI. The red dots indicate years with DAI above the average of the entire series (red dashed line) and the blue ones below. (For interpretation of the references to colour in this figure legend, the reader is referred to the Web version of this article.)

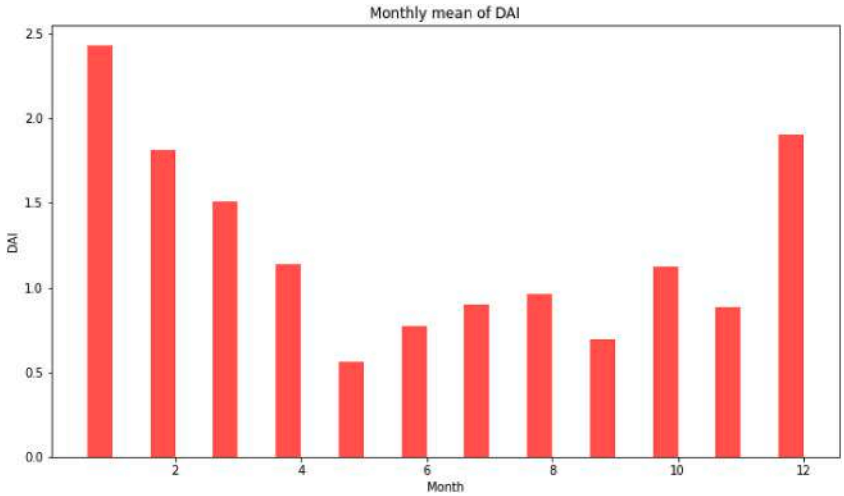

Fig. 12. Monthly average of DAI.

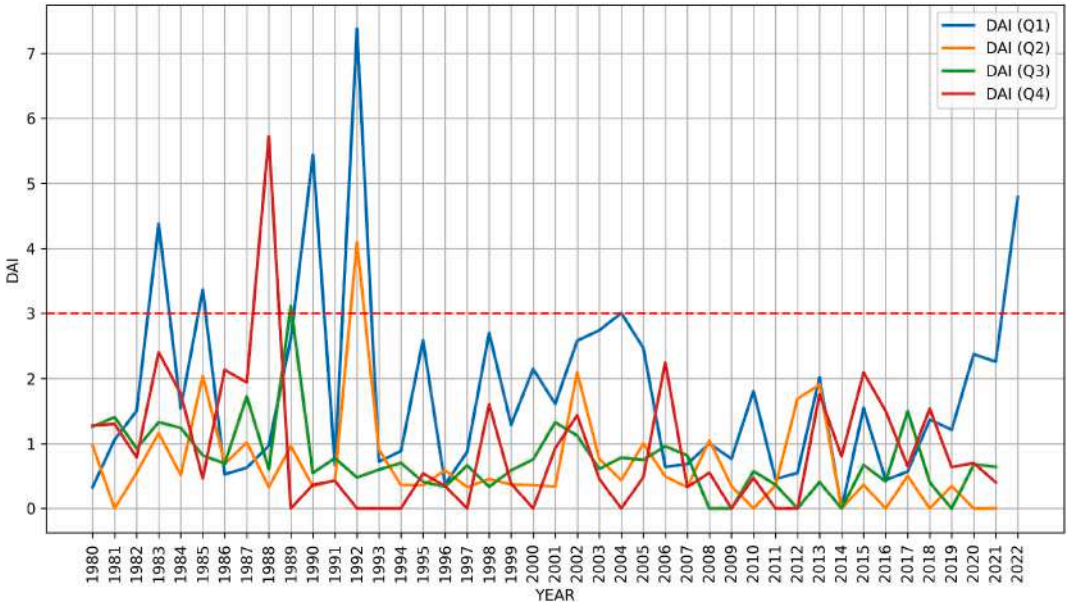

Fig. 13. Seasonal evolution of DAI.

pressure system is located north of the Iberian Peninsula, while the low cut-off is situated to the west of the Canary Islands. In the rest of the year it was observed that the geopotential anomalies were less marked, especially in the Q3 quarter

- In order to know and compare the dust events and determine which have been the most severe, the DAI was calculated. The DAI average throughout the entire period analyzed is 1.27 and only 4 events of the 483 registered show DAI values greater than 10. These most intense dust events based on DAI have been January 03, 1992, December 27, 1988, January 17, 1983 and January 28, 2022. Monthly it is observed that the maximum of DAI occurs in January and the minimum in May. On a quarterly basis, the Q1 quarter posted the highest average DAI values. It is precisely in Q1 when the most exceedances of the DAI = 3 (in the Q1 of 5 years the DAI = 3 has been exceeded) threshold have occurred throughout the study period.

Data availability statement

Data will be made available on request.

CRediT authorship contribution statement

D. Suárez-Molina: Writing – original draft, Visualization, Software, Methodology, Investigation, Formal analysis, Data curation, Conceptualization. **E. Cuevas:** Methodology, Investigation, Conceptualization. **S. Alonso-Pérez:** Writing – review & editing, Visualization, Software. **L. Cana:** Writing – review & editing, Supervision. **G. Montero:** Writing – review & editing, Supervision. **A. Oliver:** Writing – review & editing.

Declaration of competing interest

The authors declare that they have no known competing financial interests or personal relationships that could have appeared to influence the work reported in this paper.

Acknowledgments

The authors would like to thank the staff of the Operational Climatological Applications Area (ACAO) of AEMET for their day-to-day work in maintaining the National Climatic Data Bank. We would also like to thank the Aeronautical Observers at the airports, as without their professionalism this work would not have been possible. We would also like to thank the anonymous reviewers, whose comments have considerably improved the manuscript.

References

[1] S. Kinne, M. Schulz, C. Textor, S. Guibert, Y. Balkanski, S.E. Bauer, T. Berntsen, T.F. Berglen, O. Boucher, M. Chin, W. Collins, F. Dentener, T. Diehl, R. Easter, J. Feichter, D. Fillmore, S. Ghan, P. Ginoux, S. Gong, A. Grini, J. Hendricks, M. Herzog, L. Horowitz, I. Isaksen, T. Iversen, A. Kirkevåg, S. Kloster, D. Koch, J. E. Kristjansson, M. Krol, A. Lauer, J.F. Lamarque, G. Lesins, X. Liu, U. Lohmann, V. Montanaro, G. Myhre, J. Penner, G. Pitari, S. Reddy, O. Seland, P. Stier,

T. Takemura, X. Tie, An AeroCom initial assessment – optical properties in aerosol component modules of global models, Atmos. Chem. Phys. 6 (2006) 1815–1834, https://doi.org/10.5194/acp-6-1815-2006.
[2] N. Huneeus, O. Boucher, F. Chevallier, Atmospheric inversion of SO2 and primary aerosol emissions for the year 2010, Atmos. Chem. Phys. 13 (2013) 6555–6573.
[3] J.F. Kok, D.A. Ridley, Q. Zhou, R.L. Miller, C. Zhao, C.L. Heald, D.S. Ward, S. Albani, K. Haustein, Smaller desert dust cooling effect estimated from analysis of dust size and abundance, Nat. Geosci. 10 (2017) 274–278.
[4] P. Ginoux, J.M. Prospero, T.E. Gill, N.C. Hsu, M. Zhao, Global-scale attribution of anthropogenic and natural dust sources and their emission rates based on MODIS Deep Blue aerosol products, Rev. Geophys. 2012 (2012) 50.
[5] J.F. Kok, A.A. Adebiyi, S. Albani, Y. Balkanski, R. Checa-Garcia, M. Chin, P.R. Colarco, D.S. Hamilton, Y. Huang, A. Ito, M. Klose, L. Li, N.M. Mahowald, R. L. Miller, V. Obiso, C. Pérez García-Pando, A. Rocha-Lima, J.S. Wan, Contribution of the world's main dust source regions to the global cycle of desert dust, Atmos. Chem. Phys. 21 (2021) 8169–8193, https://doi.org/10.5194/acp-21-8169-2021.
[6] J.M. Prospero, P.J. Lamb, African droughts and dust transport to the Caribbean:climate change implications, Science 302 (2003) 1024e1027, https://doi.org/10.1126/science.1089915.
[7] J. Díaz, A. Tobías, C. Linares, Saharan dust and association between particulate matter and case-specific mortality: a case crossover analysis in Madrid (Spain), Environ. Health 11 (2012) 1–6, https://doi.org/10.1186/1476-069X-11-11, 2012.
[8] A. Karanasiou, N. Moreno, T. Moreno, M. Viana, F. de Leeuw, X. Querol, Health effects from Sahara dust episodes in Europe: literature review and research gaps, Environ. Int. 47 (2012) 107e114.
[9] G.R. Foltz, M.J. McPhaden, Impact of Saharan dust on tropical north Atlantic SST, J. Clim. 21 (2008) 5048e5060.
[10] I. Tegen, R. Torres, Global iron connections: desert dust, ocean biogeochemistry and climate, Science 308 (2005) 67e71.
[11] J.M. Prospero, Long-range transport of mineral dust in the global atmosphere: impact of African dust on the environment of the southeastern United States, Proc. Natl. Acad. Sci. USA 96 (7) (1999) 3396e3403, https://doi.org/10.1073/pnas.96.7.3396.
[12] J.M. Prospero, F.-X. Collard, J. Molinié, A. Jeannot, Characterizing the annual cycle of African dust transport to the Caribbean Basin and South America and its impact on the environment and air quality, Glob. Biogeochem. Cycles 29 (2014), https://doi.org/10.1002/2013GB004802.
[13] E. Cuevas, C. Milford, A. Barreto, J.J. Bustos, R.D. García, C.L. Marrero, N. Prats, C. Bayo, R. Ramos, E. Terradellas, D. Suárez, S. Rodríguez, J. de la Rosa, J. Vilches, S. Basart, E. Werner, E. López-Villarrubia, S. Rodríguez-Mireles, M.L. Pita Toledo, O. González, J. Belmonte, R. Puigdemunt, J.A. Lorenzo, P. Oromí, R. del Campo-Hernández, Desert dust Outbreak in the canary islands (February 2020): assessment and impacts, in: E. Cuevas, C. Milford, S. Basart (Eds.), State Meteorological Agency (AEMET), Madrid, Spain and World Meteorological Organization, WMO Global Atmosphere Watch (GAW), Geneva, Switzerland, 2021. Report No. 259, WWRP 2021-1.
[14] M.V. Sivakumar, Impacts of sand storms/dust storms on agriculture, in: Natural Disasters and Extreme Events in Agriculture, Springer, Berlin, Heidelberg, 2005, pp. 159–177.
[15] T.D. Jickells, Z.S. An, K.K. Andersen, A.R. Baker, G. Bergametti, N. Brooks, J.J. Cao, P.W. Boyd, R.A. Duce, K.A. Hunter, H. Kawahata, N. Kubilay, J. laRoche, P. S. Liss, N. Mahowald, J.M. Prospero, A.J. Ridgwell, I. Tegen, R. Torres, Global iron connections between desert dust, ocean biogeochemistry, and climate, Science 308 (5718) (2005) 67–71.
[16] O. Boucher, D. Randall, P. Artaxo, C. Bretherton, G. Feingold, P. Forster, V.-M. Kerminen, Y. Kondo, H. Liao, U. Lohmann, P. Rasch, S.K. Satheesh, S. Sherwood, B. Stevens, X.Y. Zhang, Clouds and aerosols, in: T.F. Stocker, D. Qin, G.-K. Plattner, M. Tignor, S.K. Allen, J. Doschung, A. Nauels, Y. Xia, V. Bex, P.M. Midgley (Eds.), Climate Change 2013: the Physical Science Basis. Contribution of Working Group I to the Fifth Assessment Report of the Intergovernmental Panel on Climate Change, Cambridge University Press, 2013, pp. 571–657. https://www.cambridge.org/core/books/climate-change-2013-the-physical-sciencebasis/clouds-and-aerosols/11F2D995DB0981610675738B72E7AECA.
[17] E. Terradellas, S. Nickovic, X. Zhang, Airborne dust: a hazard to human health, environment and society, World Meteorol. Organ. Bull. 64 (2015).
[18] WMO, in: S. Nickovic, E. Cuevas, J. Baldasano, E. Terradellas, T. Nakazawa, A. Baklanov (Eds.), Sand and Dust Storm Warning Advisory and Assessment System (SDS–WAS): Science and Implementation Plan 2015–2020, World Meteorological Organization, Geneva, 2015, p. 37. WWRP Report 2015 – 5, http://www.wmo.int/pages/prog/arep/wwrp/new/documents/Final_WWRP_2015_5_SDS_IP.pdf.
[19] D. Meloni, A. di Sarra, F. Monteleone, G. Pace, S. Piacentino, D.M. Sferlazzo, Seasonal transport patterns of intense Saharan dust events at the Mediterranean island of Lampedusa, 2008, Atmos. Res. 88 (2) (2008) 134–148, https://doi.org/10.1016/j.atmosres.2007.10.007. ISSN 0169-8095.
[20] H. Cao, C. Fu, W. Zhang, J. Liu, Characterizing sand and dust storms (SDS) intensity in China based on meteorological data, Sustainability 10 (2018) 2372, https://doi.org/10.3390/su10072372.
[21] P. Dorta, Catálogo de riesgos climáticos en Canarias: Amenazas y vulnerabilidad, Geographicalia 51 (2007) 133–160.
[22] S. Feuerstein, K. Schepanski, Identification of dust sources in a saharan dust hot-spot and their implementation in a dust-emission model, Rem. Sens. 11 (1) (2019) 4, https://doi.org/10.3390/rs11010004.
[23] I. Font Tullot, El tiempo atmosférico en las islas Canarias, Servicio Meteorológico Nacional. Serie A 26 (1956) (Instituto Nacional de Meteorología), http://hdl.handle.net/20.500.11765/9616.
[24] J.M. y Prospero, T.N. Carlson, Vertical and real distribution of Saharan dust over the western ecuatorial North Atlantic Ocean, J. Geophys. Res. 77 (1972) 5255–5265.
[25] G. Bergametti, L. Gomes, G. Coudé-Gaussen, P.Y. Rognon, M.N.L. Coustumer, African dust observed over Canary Islands: source regions identification and transport pattern for some summer situation, J. Geophys. Res. 94 (1989) 14855–14864.
[26] I. Chiapello, G. Bergametti, L. y Gomes, B. Chatenet, An additional low layer transport of Sahelian and Saharan dust over the North-Eastern Tropical Atlantic, Geophys. Res. Lett. 22 (23) (1995) 3191–3194.
[27] E. Cuevas, Estudio del comportamiento del ozono troposférico en el observatorio de Izaña y su relación con la dinámica atmosférica. Tesis Doctoral. Facultad de Ciencias Físicas, Universidad Complutense de Madrid, 1995.
[28] J.J. Bustos, E. Cuevas, C. Marrero, S. y Alonso, Caracterización de las masas de aire en la troposfera libre y en la capa de mezcla en Canarias. Proceedings de la IX Asamblea de Geodesia y Geofísica, 1998, pp. 9–13. Aguadulce (Almería).
[29] S. Rodríguez, Comparación de las variaciones de ozono superficial asociadas a procesos de transporte sobre y bajo la inversión de temperatura subtropical en Tenerife, Tesis de Licenciatura, Universidad de La Laguna (1999).
[30] S. Rodríguez, J.C. Gerra, Monitoring of ozone in a marine environment in Tenerife (canary islands), Atmos. Environ. 135 (2001) 18291841.
[31] C.J. Torres, E. Cuevas, J.C. Guerra, V. y Carreño, Caracterización de las Masas de Aire en la Región Subtropical. Proceedings del V Simposio Nacional de Predicción, Instituto Nacional de Meteorología, Madrid, 2001, pp. 20–23. Noviembre, 2001.
[32] M. Viana, Niveles, composición y origen del material particulado atmosférico en los sectores Norte y Este de la Península Ibérica y Canarias. Tesis Doctoral. Consejo Superior de Investigaciones Científicas, Universitat de Barcelona, 2003.
[33] P. Dorta, M.D. Gelado, J.J. Hernández, P. Cardona, C. Collado, S. Mendoza, M.J. Rodríguez, V. Siruela, M.E. Torres, Frecuencia, estacionalidad y tendencias de las advecciones de aire sahariano en Canarias (1976-2003), Invest. Geográficas nº38 (2005) (2005) 23–45. Instituto Universitario de Geografía. Universidad de Alicante.
[34] S. Alonso-Pérez, E. Cuevas, X. Querol, Objective identification of synoptic meteorological patterns favouring African dust intrusions into the marine boundary layer of the subtropical eastern north Atlantic region, Meteorol. Atmos. Phys. 113 (2011) 109–124.
[35] M. Viana, X. Querol, A. Alastuey, E. y Cuevas, S. Rodríguez, Influence of African dust on the levels of atmospheric particulates in the Canary Islands air quality network, Atmos. Environ. 36 (2002) 5861–5875.
[36] Markus Kottek, Jürgen Grieser, Christoph Beck, Bruno Rudolf, Franz Rubel, World Map of the Köppen-Geiger climate classification updated, Meteorol. Z. 15 (3) (2006) 259–263, https://doi.org/10.1127/0941-2948/2006/0130. Bibcode:2006MetZe.15.259K.
[37] AEMET, Atlas climático de los archipiélagos de Canarias, Madeira y Azores, vol. 2012, Ministerio de Agricultura, Alimentación y Medio Ambiente, 2012, https://doi.org/10.31978/281-12-006-X. NIPO: 281-12-006-X.

[38] I. Font Tullot, Climatología de España y Portugal, Instituto Nacional de Meteorología, 1983. ISBN: 978-84-5009-467-4.
[39] WMO-No. 488. Guide to the Global Observing System. Part III, 3.2.2.2.4 Visibility.
[40] WMO-No. 731. Guide to Meteorological Observing and Information Distribution Systems for Aviation Weather Services.
[41] E. Kalnay, M. Kanamitsu, R. Kistler, W. Collins, D. Deaven, L. Gandin, M. Iredell, 1 S. Saha, G. White, J. Woollen, Y. Zhu, A. Leetmaa, R. Reynolds, M. Chelliah, W. Ebisuzaki, W. Higgins, J. Janowiak, K.C. Mo, C. Ropelewski, J. Wang, R. Jenne, D. Joseph, 3 the NCEP/NCAR 40-year reanalysis project, B. Am. Meteorol. Soc. 77 (1996) 437–471.
[42] ICAO, Manual of Aeronautical Meteorological Practice (Doc 8896), International Civil Aviation Organization, 2021. Thirteenth Edition, 2021.
[43] H.B. Mann, Nonparametric tests against trend, Econometrica 13 (1945) 245–259.
[44] M.G. Kendall, Rank Correlation Methods, fourth ed., Charles Griffin, London, 1975.
[45] R.O. Gilbert, Statistical Methods for Environmental Pollution Monitoring, Wiley, NY, 1987.
[46] K.W. Hipel, A.I. McLeod, Time series modelling of water resources and environmental systems. Electronic reprint of our book orginally published in 1994. http://www.stats.uwo.ca/faculty/aim/1994Book/, 2005.
[47] M.C. Baddock, C.L. Strong, J.F. Leys, S.K. Heidenreich, E.K. Tews, G.H. McTainsh, A visibility and total suspended dust relationship, Atmos. Environ., Volume 89, 14, Pages 329-336, ISSN 1352-2310.https://doi.org/10.1016/j.atmosenv.2014.02.038.
[48] A.D. Boloorani, Contingency Planning Process for Catalysing Investments and Actions to Enhance Resilience against Sand and Dust Storms in Agriculture in the Islamic Republic of Iran, FAO, Rome, 2023, https://doi.org/10.4060/cc8401en.
[49] Waleed Hamza, Mohamed Rizk Enan, Huda Al-Hassini, Jan-Berend Stuut, Dirk de-Beer, Dust storms over the Arabian Gulf: a possible indicator of climate changes consequences, Aquat. Ecosys. Health Manag. 14 (3) (2011) 260–268, https://doi.org/10.1080/14634988.2011.601274.
[50] O'LoingsighT., McTainsh G.H., Tews E.K., Strong C.L., Leys J.F., Shinkfield P., Tapper N.J.,The Dust Storm Index (DSI): A method for monitoring broadscale wind erosion using meteorological records,Aeolian Research,Volume 12,2014,Pages 29-40,ISSN 1875-9637,https://doi.org/10.1016/j.aeolia.2013.10.004.
[51] J.B. MacQueen, Some methods for classification and analysis of multivariate observations, in: Proceedings of 5th Berkeley Symposium on Mathematical Statistics and Probability, vol. 1, University of California Press, 1967, pp. 281–297. MR 0214227. Zbl 0214.46201.
[52] N.M. Mahowald, J.A. Ballantine, J. Feddema, N. Ramankutty, Global trends in visibility: implications for dust sources, Atmos. Chem. Phys. 7 (12) (2007) 3309–3339.
[53] Xin Xi, Revisiting the recent dust trends and climate drivers using horizontal visibility and present weather observations, J. Geophys. Res. Atmos. 126 (2021), https://doi.org/10.1029/2021JD034687.
[54] I. Chiapello, C. Moulin, J.M. Prospero, Understanding the long-term variability of African dust transport across the Atlantic as recorded in both Barbados surface concentrations and large-scale Total Ozone Mapping Spectrometer (TOMS) optical thickness, J. Geophys. Res. Atmos. 110 (D18) (2005).
[55] A.T. Evan, C. Flamant, M. Gaetani, F. Guichard, The past, present and future of African dust, Nature 531 (7595) (2016) 493–495.
[56] D. Suárez Molina, C. Marrero, E. Cuevas Agulló, E. Werner, N. Prats Porta, S. Basart, Caracterización de las Intrusiones de Polvo en Canarias, Agencia Estatal de Meteorología, Madrid, Spain, 2021.
[57] Á. Barreto, E. Cuevas, R.D. García, J. Carrillo, J.M. Prospero, L. Ilić, M. Yela, Long-term characterisation of the vertical structure of the Saharan Air Layer over the Canary Islands using lidar and radiosonde profiles: implications for radiative and cloud processes over the subtropical Atlantic Ocean, Atmos. Chem. Phys. 22 (2) (2022) 739–763.